JPET Fast Forward. Published on May 26, 2017 as DOI: 10.1124/jpet.117.241703
This article has not been copyedited and formatted. The final version may differ from this version.

JPET #241703

Potential drug interactions mediated by renal organic anion transporter OATP4C1

Toshihiro Sato, Eikan Mishima, Nariyasu Mano, Takaaki Abe, Hiroaki Yamaguchi

Department of Pharmaceutical Sciences, Tohoku University Hospital (T.S., N.M., H.Y.)

Division of Nephrology, Endocrinology, and Vascular Medicine, Tohoku University, Graduate School of Medicine (E.M., T.A.)

Division of Medical Science, Tohoku University, Graduate School of Biomedical Engineering (T.A.)

Department of Clinical Biology and Hormonal Regulation, Tohoku University, Graduate School of Medicine (T.A.)

JPET Fast Forward. Published on May 26, 2017 as DOI: 10.1124/jpet.117.241703
This article has not been copyedited and formatted. The final version may differ from this version.

Running title; Potential drug interactions via OATP4C1

Corresponding author:

Hiroaki Yamaguchi, Ph.D.

E-mail address: yamaguchi@hosp.tohoku.ac.jp

Tel: 81-22-717-7528

Fax: 81-22-717-7545

The number of

text pages; 32

tables; 1

figures; 3

references; 44

The number of words in the

Abstract; 249

Introduction; 333

Discussion; 1297

Abbreviations

ABC : ATP-binding cassette

CKD : Chronic kidney disease

DAPI : 4',6-Diamidino-2-phenylindole

DDI : Drug-drug interaction

HPLC : High performance liquid chromatography

IC_{50} : Half maximal (50%) inhibitory concentration

IgG : Immunoglobulin G

IS : Internal standard

KH buffer : Krebs-Henseleit buffer

LC/MS/MS : Liquid chromatography/tandem mass spectrometry

MATE : Multidrug and toxic compound extrusion

NGS : Normal goat serum

OAT : Organic anion transporter

OATP : Organic anion transporting polypeptide

OCT : Organic caion transporter

PBPK : Physiologically based pharmacokinetic

PBS : Phosphate-buffered saline

P-gp : P-glycoprotein

PVDF : Polyvinylidene fluoride

RIPA : Radio immunoprecipitation assay

JPET Fast Forward. Published on May 26, 2017 as DOI: 10.1124/jpet.117.241703
This article has not been copyedited and formatted. The final version may differ from this version.

SDS-PAGE : Sodium dodecyl sulphate polyacrylamide gel electrophoresis

SRM : Selected reaction monitoring

T_3 : Triiodothyronine

TBS : Tris-buffered saline

Abstract

OATP4C1 is an organic anion transporter expressed in the basolateral membrane of the renal proximal tubules. It plays a major role in the urinary excretion of both exogenous drugs and endogenous compounds. Our previous studies have indicated the importance of OATP4C1 in pathological and physiological conditions; however, the majority of its pharmacological characteristics remained unclear. Therefore, to provide essential information for clinical drug therapy decisions and drug development, we, in this study, attempted to clarify drug interactions mediated by OATP4C1. To elucidate potential drug interactions via OATP4C1, we screened 53 representative drugs, which are commonly used in clinical settings. Next, we evaluated IC_{50} values of drugs which inhibited OATP4C1 by more than 50%. To apply our results to clinical settings, we calculated the drug-drug interaction (DDI) indices. The screening analysis using an OATP4C1-expressing cell system demonstrated that 22 out of 53 therapeutic drugs inhibited OATP4C1-mediated T_3 transport. In particular, OATP4C1-mediated transport was strongly inhibited by 10 drugs. The IC_{50} values of 10 drugs; nicardipine, spironolactone, fluvastatin, crizotinib, levofloxacin, clarithromycin, ritonavir, saquinavir, quinidine, and verapamil, obtained in this study were 51, 53, 41, 24, 420, 200, 8.5, 4.3, 100, and 110 μM, respectively. The IC_{50} values of these drugs were higher than plasma concentrations obtained in clinical practice. However, ritonavir showed the highest DDI index (1.9) for OATP4C1, suggesting that it may strongly influence this transporter and thus cause drug interactions that are seen in clinical settings. Our finding gives new insight into the role of OATP4C1 in clinical DDIs.

JPET Fast Forward. Published on May 26, 2017 as DOI: 10.1124/jpet.117.241703
This article has not been copyedited and formatted. The final version may differ from this version.

Introduction

The kidney plays an important role in the excretion of endogenous and exogenous compounds by moving them from the blood into the urine. Urinary excretion involves two main processes – glomerular filtration and tubular secretion. Renal tubular secretion is mediated by membrane transporters expressed in the proximal tubules including the organic anion transporting polypeptide (OATP) family, the organic anion transporter (OAT) family, organic cation transporter (OCT) family, multidrug and toxic compound extrusion (MATE) family, and ATP-binding cassette (ABC) family.

OATPs are sodium-independent organic anion transporters found in a variety of tissues, including the liver, kidney, intestines, and brain. OATPs contribute to the transport of bile acids, thyroid hormones, steroid conjugates, anionic oligopeptides, eicosanoids, various drugs, and other xenobiotic compounds across membranes (Hagenbuch and Meier, 2003; Hagenbuch and Meier, 2004; Kullak-Ublick et al., 2004; Mikkaichi et al., 2004a; Sato et al., 2014; Sato et al., 2017; Suga et al., 2017).

OATP4C1 is the first member of the OATP family found to be predominantly expressed in the kidney. OATP4C1 is localized in the basolateral membrane of the proximal tubule, and plays a major role in urinary secretion of cardiac glycosides (digoxin and ouabain), thyroid hormones [triiodothyronine (T_3) and thyroxine], cAMP, methotrexate, sitagliptin, estrone 3-sulphate, chenodeoxycholic acid, and glycocholic acid (Mikkaichi et al., 2004b; Chu et al., 2007; Yamaguchi et al., 2010). Moreover, our previous study suggested that estrone 3-sulphate does not bind to the recognition site for digoxin in the OATP4C1 molecule (Yamaguchi et al., 2010).

JPET Fast Forward. Published on May 26, 2017 as DOI: 10.1124/jpet.117.241703
This article has not been copyedited and formatted. The final version may differ from this version.

Toyohara et al. showed that overexpression of human *SLCO4C1*, which encodes OATP4C1 in a rat model of chronic kidney disease (CKD) ameliorated the progression of renal damage, hypertension, cardiomegaly, and inflammation by reducing the accumulation of uremic toxins such as guanidino succinate, asymmetric dimethylarginine, and *trans*-aconitate (Toyohara et al., 2009). However, pharmacological characteristics of OATP4C1 such as drug-drug interactions (DDIs) are not well studied. In the present study, in order to provide essential information for drug therapy and drug development, we attempted to clarify clinically relevant drug interactions via OATP4C1.

Materials and methods

Materials

Triiodothyronine (T_3) and sodium butyrate were purchased from Nacalai Tesque, Inc. (Kyoto, Japan). All other chemicals were commercially available and of the highest purity possible.

Cell culture and establishment of OATP4C1 stably expressing cells

MDCKII cells were cultured in Dulbecco's modified Eagle's medium supplemented with 10% foetal bovine serum under an atmosphere of 5% CO_2 and 95% air at 37°C. Cells were transfected with a *pcDNA3.1*(+) plasmid vector (ThermoFisher Scientific, Waltham, MA) encoding OATP4C1 using Lipofectamine® 3000 (ThermoFisher Scientific) according to the manufacturer's instructions. After three weeks of selection in G418 (0.5 mg/mL), we screened

single colonies for OATP4C1 expression by transport studies. Cells transfected with the empty vector were used as controls.

Western blotting

Cells were lysed in radio immunoprecipitation assay (RIPA) buffer (Santa Cruz Biotechnology, Santa Cruz, CA). The protein content of the solubilized cells was determined by the Bradford method using a Protein Assay kit (Bio-Rad Laboratories Inc., Hercules, CA) with bovine serum albumin used as a standard. Fifty micrograms of protein were subjected to sodium dodecyl sulphate polyacrylamide gel electrophoresis (SDS-PAGE) and then transferred to Immun-Blot polyvinylidene fluoride (PVDF) membranes (Bio-Rad Laboratories, Hercules, CA). Blots were blocked by 5% skim milk in tris-buffered saline (2 mM Tris, 138 mM NaCl, pH 7.6) containing 0.1% Tween 20 (TBS-T) at room temperature for 30 min, and then probed with anti-human SLCO4C1 antibody (1:1000 dilution) (#HPA036516, Sigma-Aldrich, St. Louis, MO) at 4°C overnight. The blots were washed and then incubated with goat anti-rabbit immunoglobulin G (IgG) conjugated with horseradish peroxidase (1:1000 dilution, PIERCE, Rockford, IL). ECL™ plus chemiluminescent system (GE Healthcare UK Ltd, Little Chalfont, England) was used for detection.

Immunohistochemistry

Mock and OATP4C1-expressing MDCKII cells were fixed with 10% formaldehyde neutral buffer solution (Nacalai Tesque, Inc., Kyoto). After incubation in phosphate-buffered

JPET Fast Forward. Published on May 26, 2017 as DOI: 10.1124/jpet.117.241703
This article has not been copyedited and formatted. The final version may differ from this version.

saline containing 0.1% Triton-X100 (PBS-T) at room temperature for 5 min, the specimens were blocked with 3% normal goat serum (NGS) in PBS at room temperature for 10 min, and then probed with anti-human SLCO4C1 antibody (1:100 dilution) in PBS containing 3% NGS (#HPA036516, Sigma-Aldrich, St. Louis, MO) at 4°C overnight. The specimens were then incubated with CF594 F(ab′)2 fragment of goat anti-rabbit IgG (1:500 dilution, Biotium, Fremont, CA) in PBS containing 3% NGS at room temperature for 1 hour. For immunofluorescent microscopy, cells were double stained with the nucleus marker 4',6-diamidino-2-phenylindole (DAPI). After washing with PBS and fixing by mounting medium, images were taken with a $C2^{+}$ laser confocal microscope system (Nikon Corporation, Tokyo, Japan).

Transport studies

The cellular uptake in monolayer cultures grown on 24-well plates was measured. After washing once, the cells were pre-incubated in Krebs-Henseleit (KH) buffer (118 mM NaCl, 23.8 mM $NaHCO_3$, 4.83 mM KCl, 0.96 mM KH_2PO_4, 1.20 mM $MgSO_4$, 12.5 mM *N*-(2-hydroxyethyl) piperazine-*N*′-2-ethanesulphonic acid, 5.0 mM D-glucose, and 1.53 mM $CaCl_2$, pH 7.4). Uptake was initiated by adding T_3 with or without any of the trial drugs. At the indicated times, uptake was terminated by replacing the uptake buffer with ice-cold KH buffer and then washing twice with ice-cold KH buffer. Concentration of T_3 was measured by liquid chromatography/tandem mass spectrometry (LC/MS/MS). The uptake was calculated by dividing the uptake amount by the protein amount of the cells.

JPET Fast Forward. Published on May 26, 2017 as DOI: 10.1124/jpet.117.241703
This article has not been copyedited and formatted. The final version may differ from this version.

Inhibitory effects of various therapeutic drugs

We calculated IC_{50} values of drugs that inhibited OATP4C1-mediated uptake of T_3 by over 50%. The IC_{50} values were estimated using a nonlinear least-squares regression analysis of the competition curves. The following equation was used:

$$V = \frac{100 \times IC_{50}{}^{n}}{IC_{50}{}^{n} + [I]^{n}} \quad (1)$$

where V is the transport amount (% of control), $[I]$ is the drug concentration, and n is the Hill coefficient.

Drug-drug interaction index prediction

To relate our findings to clinical applications, we calculated the DDI index (Izumi et al., 2015; FDA, 2012; Ito et al., 1998) according to FDA guideline. We used the maximum plasma concentration (C_{max}) and the maximum concentration of unbound drug in the plasma ($C_{max,u}$) for each drug, along with the IC_{50} values from our *in vitro* study to predict the possibility of a clinical DDI according to the following equation (FDA, 2012; Ito et al., 1998; Parvez et al., 2016; Pan et al., 2013; Chioukh et al., 2014; Lau et al., 2007):

$$\text{DDI index} = \frac{C_{max}}{IC_{50}} \text{ or } \frac{C_{max,u}}{IC_{50}} \quad (2)$$

Quantification of T_3 by LC/MS/MS

Cells were scraped and homogenized in 200 μL of water for T_3 analysis. Cell lysates were de-proteinized by adding equal volumes of acetonitrile containing internal standard (IS). The

JPET Fast Forward. Published on May 26, 2017 as DOI: 10.1124/jpet.117.241703
This article has not been copyedited and formatted. The final version may differ from this version.

mixture was vortexed and centrifuged at 15,000 × *g* for 5 min at room temperature. The supernatant was used directly for measurement. Chromatographic separation was carried out using a Shimadzu Nexera HPLC System (Shimadzu, Kyoto) with a Cosmosil $5C_{18}$-MS-II column (50 mm × 2.0 mm i.d., 5 μm, Nacalai Tesque, Inc., Kyoto). To determine T_3 concentration, the column was eluted with an isocratic flow of acetonitrile/water/acetic acid (30:70:0.1, v/v/v) at a flow rate of 0.2 mL/min. The injection volume was 5 μL and the column temperature was maintained at 40°C. Positive and negative ion electrospray tandem mass spectrometric analysis was carried out using a TSQ Vantage EMR LC/MS/MS System (Thermo Scientific, Waltham, MA) at unit resolution with selected reaction monitoring (SRM). SRM transitions monitored were *m/z* 652 > 606 for T_3 (ESI+) and *m/z* 423 > 101 for pravastatin (IS, ESI-). Data were acquired and analysed using Xcalibur™ software (version 2.1, Thermo Scientific).

Statistical analysis

Data are expressed as mean ± standard error (S.E.). When appropriate, the differences between groups were tested for significance using the unpaired Student's t-test. Statistical significance was indicated by *p* values less than 0.05.

Results

Establishment of OATP4C1 stably expressing cells

First, we have tried to establish OATP4C1 expressing cells by using the human kidney derived cell lines (HK-2, ACHN, HEK293, etc.). But unfortunately, OATP4C1 expressed human

cell lines could not be established with those cell lines. To examine the transport study of OATP4C1, we could establish a human OATP4C1-stably expressing cell system using canine renal tubule derived-MDCKII cells by following previous reports (Mikkaichi et al., 2004b, Yamaguchi et al., 2010). After selection with G418, single colonies for OATP4C1 expression were screened by transport studies. First, we examined the transport of triiodothyronine (T_3), which is a well-known substrate of OATP4C1. T_3 was significantly transported by several OATP4C1-expressing clones than by empty vector-transfected control cells. Because, among those clones, No. 68 (hereafter referred to at OATP4C1/MDCKII cells) exhibited the highest OATP4C1 transport activity, we used this clone for the rest of the analysis. We observed that sodium butyrate treatment significantly enhanced OATP4C1-mediated T_3 uptake (Fig. 1A). Sodium butyrate treatment (5 mM, 24hr) was adopted referring to previous reports (Chen et al., 2007; Yang et al., 2009; Lu et al., 2013). We then tried to characterize the transport of T_3 by OATP4C1 in the presence of sodium butyrate, and observed that the time dependent transport of T_3 by OATP4C1/MDCKII cells was significantly higher than that by mock cells (Supplementary Fig. S1). After 60 minutes, levels of cellular accumulation of T_3 into OATP4C1/MDCKII cells (50 ± 0.13 pmol/mg protein) were 2.4-fold greater than that into mock cells (21 ± 0.16 pmol/mg protein). The apparent Michaelis-Menten constant (K_m) for OATP4C1-mediated T_3 uptake was 7.9 ± 1.3 μM in the presence of sodium butyrate (Supplementary Fig. S1). This value is comparable to the values previously reported by Mikkaichi et al (Mikkaichi et al., 2004b). In addition, we confirmed the cell surface expression of OATP4C1 in the OATP4C1/MDCKII cells by Western blotting and immunohistochemical analysis. Western blotting showed the specific expression of

JPET Fast Forward. Published on May 26, 2017 as DOI: 10.1124/jpet.117.241703
This article has not been copyedited and formatted. The final version may differ from this version.

OATP4C1 in OATP4C1/MDCKII cells (Fig. 1B). The protein expression amount was increased by exposure to sodium butyrate (Fig. 1B and Fig. 1C). Furthermore, immunohistochemical analysis showed the cell surface expression of OATP4C1 in the cells exposed to sodium butyrate (Fig. 1D). Since more substrate was transported in the presence of sodium butyrate, we decided to use cells exposed to it in all later experiments. Additionally, we did experiment within passage 40, and T_3 uptake by OATP4C1/MDCKII cells was stable.

Inhibitory effects of various therapeutic drugs on OATP4C1-mediated transport

To elucidate potential drug interactions via OATP4C1, we screened 53 representative drugs, which are commonly used in clinical settings (Fig. 2). We selected and evaluated both renal and hepatic excretion drugs. Most of those drugs are also reported to be transporter's substrate or inhibitor, such as organic ion transporters and ABC transporters. Inhibitor concentrations were set much higher than those in clinics (the solubility upper limit or 100 times high) to avoid overlooking the interaction. OATP4C1-mediated transport was strongly inhibited (more than 50%) by 10 drugs: nicardipine (100 μM), spironolactone (100 μM), fluvastatin (50 μM), crizotinib (50 μM), levofloxacin (1000 μM), clarithromycin (250 μM), ritonavir (100 μM), saquinavir (25 μM), quinidine (100 μM), and verapamil (100 μM) (Fig. 2). Twelve other drugs also inhibited OATP4C1-mediated transport, but the inhibition by those drugs was moderate (greater than 20%, less than 50%): celecoxib (50 μM), propranolol (100 μM), nifedipine (100 μM), furosemide (100 μM), bosentan (100 μM), gefitinib (50 μM), imatinib (100 μM), lenalidomide (100 μM), aciclovir (1000 μM), amiodarone (100 μM), cibenzoline (100 μM), and empagliflozin (100 μM) (Fig. 2).

No significant inhibition of OATP4C1-mediated transport was observed with the other 31 screened drugs (25-1000 μM) (Fig. 2).

Next, we evaluated IC_{50} values of the 10 drugs that inhibited OATP4C1 by more than 50% (equation (1), see Methods). All of these drugs inhibited OATP4C1-mediated transport in a concentration-dependent manner (Fig. 3A-J). The IC_{50} values of nicardipine, spironolactone, fluvastatin, crizotinib, levofloxacin, clarithromycin, ritonavir, saquinavir, quinidine, and verapamil for OATP4C1 were 51 ± 8, 53 ± 7, 41 ± 8, 24 ± 8, 420 ± 150, 200 ± 16, 8.5 ± 1.4, 4.3 ± 0.6, 100 ± 11, and 110 ± 22 μM, respectively.

Prediction of the DDI index

To apply our results to clinical settings, we calculated the DDI indices according to FDA guideline using the maximum concentration in plasma (C_{max}) and the unbound maximum concentration in plasma ($C_{max,u}$) (equation (2), see Methods). The DDI indices revealed that mild inhibition of OATP4C1-mediated uptake of typical substrates may occur even under normal conditions. When we estimated the inhibitory effects of ritonavir, quinidine, and saquinavir by using C_{max}, the DDI indices became significant (DDI index greater than the cut-off value of 0.1 suggested by regulatory authorities [i.e., FDA]), while levofloxacin, clarithromycin, crizotinib, spironolactone, fluvastatin, nicardipine, and verapamil showed negligible DDI indices (Table 1). The maximum DDI index of ritonavir, quinidine, and saquinavir were 1.9, 0.86, and 0.19 for OATP4C1-mediated T_3 uptake inhibition (Table 1). The calculated maximum DDI indices of levofloxacin, clarithromycin, crizotinib, spironolactone, fluvastatin, nicardipine, and verapamil

were 0.045, 0.019, 0.046, 0.0091, 0.016, 0.0053, and 0.0046, respectively, for OATP4C1-mediated T_3 uptake inhibition (Table 1). Among the tested drugs, ritonavir showed the highest DDI index for OATP4C1, indicating a strong possibility of clinical drug interactions.

Discussion

So far, several studies have revealed the impact of CYP3A-mediated metabolism, OATs and P-gp-mediated renal excretion on the pharmacokinetic alteration of drugs (Hsu et al., 1998, Ouellet et al., 1998, Schmitt et al., 2010, Vree et al., 1995, Landersdorfer et al., 2010, Laskin et al., 1982), other processes such as transcellular dynamics regulated by other transporters cannot be ignored. OCT and MATE have been also evaluated in several studies (Yonezawa et al., 2011). OATP4C1 is one of transporters which remains unknown. In the present study, we evaluated the interactions of various therapeutic drugs with the kidney specific organic anion transporter OATP4C1. This is the first report to clarify and summarize the interactions of therapeutic drugs on OATP4C1-mediated transport. While we evaluated OATP4C1-mediated T_3 uptake in the presence of sodium butyrate, the transport characteristics of T_3 by OATP4C1 were comparable to the previous report that did not use sodium butyrate (Mikkaichi et al., 2004b). Further, we confirmed OATP4C1-expression in MDCKII cells by performing Western blotting and immunohistochemical analysis. Our results show that OATP4C1 may be one of the drug transporters which explain the DDIs in clinical. This novel finding could provide essential information for drug therapy and drug development in the future.

From the screening results, we found that OATP4C1-mediated T_3 transport was inhibited by

JPET Fast Forward. Published on May 26, 2017 as DOI: 10.1124/jpet.117.241703
This article has not been copyedited and formatted. The final version may differ from this version.

22 out of 53 therapeutic drugs (Fig. 2). Among these drugs, inhibitory effects of 10 drugs on OATP4C1-mediated transport were strong (more than 50%) (Fig. 2). These ten drugs include many drugs that have been reported to be substrates or inhibitors of other drug transporters such as hepatic OATPs, organic ion transporters, and ABC transporters in the kidney (Supplementary Table S1). Another 12 drugs also inhibited OATP4C1-mediated transport, but the inhibition by those drugs was moderate (greater than 20%, less than 50%) (Fig. 2). As our previous study showed that OATP4C1 has multiple binding sites for its substrate (Yamaguchi et al., 2010), if other OATP4C1 substrates besides T_3 had been used in the drug screening different results may have been observed. Estrone 3-sulfate and digoxin are also reported to be substrates of OATP4C1 (Mikkaichi et al., 2004b, Yamaguchi et al., 2010). We also found that these compounds were transported by established OATP4C1/MDCKII cells in this study. However, OATP4C1 mediated estrone 3-sulfate and digoxin uptake are less than OATP4C1 mediated T_3 transport and it was difficult to evaluate the inhibition of therapeutic drugs by using those substrates in this study. Further study is needed to obtain more information about OATP4C1 interactions with therapeutic drugs.

Next, we evaluated IC_{50} values of the 10 drugs that showed strong inhibition, all of which inhibited OATP4C1-mediated transport in a concentration-dependent manner (Fig. 3A-J). The IC_{50} values of nicardipine, spironolactone, fluvastatin, crizotinib, levofloxacin, clarithromycin, ritonavir, saquinavir, quinidine, and verapamil obtained in this study were 51, 53, 41, 24, 420, 200, 8.5, 4.3, 100, and 110 μM, respectively. The IC_{50} values of these drugs were higher than plasma concentrations obtained in clinical practice (Table 1). Additionally, the IC_{50} values of

clarithromycin, levofloxacin, nicardipine, and quinidine were higher than those of hepatic OATPs, organic ion transporters, and ABC transporters expressed in proximal tubular cells (Supplementary Table S1). Crizotinib, fluvastatin, ritonavir, saquinavir, and verapamil showed equivalent or higher affinity to OATP4C1 than to those transporters located in the liver and kidney (Supplementary Table S1).

Additionally, we attempted to estimate the DDI indices and apply our results to clinical settings according to FDA guideline. As expected, the DDI indices of those drugs were not significant (DDI index less than 0.1) under normal conditions. However, when we estimated the inhibitory effects of ritonavir, quinidine, and saquinavir by using C_{max}, the DDI indices were significant (DDI index greater than 0.1), while levofloxacin, clarithromycin, crizotinib, spironolactone, fluvastatin, nicardipine, and verapamil showed negligible DDI indices. When we estimated the effect of the drugs on drug transporters, the fraction that was not protein-bound had to be taken into consideration. Among the drugs evaluated in this study, many are more than 90% protein-bound in plasma (Table 1). Thus, the effects of those drugs on OATP4C1 are thought to be small under normal conditions. However, in chronic disease states, such as chronic hepatic dysfunction and CKD, the DDI indices of drugs should be higher because of an increased proportion of unbound drugs. Furthermore, patients with chronic hepatic dysfunction or CKD frequently have hypoalbuminemia, which also results in an increase in protein-unbound drugs (Viani et al., 1989; Meijers et al., 2008). It has also been reported that compared to control subjects, dialysis patients have significantly lower levels of albumin (Małgorzewicz et al., 2008). For example, plasma concentration of fluvastatin is reported to be increase in patients with

JPET Fast Forward. Published on May 26, 2017 as DOI: 10.1124/jpet.117.241703
This article has not been copyedited and formatted. The final version may differ from this version.

hepatic dysfunction comparing to healthy subjects (C_{max} 683 μg/L (1.7 μM) vs. 269 μg/L (0.65 μM)) (Scripture and Pieper, 2001). In addition, plasma albumin concentration is reported to decrease to 3.2 g/dL (cirrhosis) and 2.3 g/dL (sepsis) (vs. healthy 4.8 g/dL) (Oettl et al., 2013). It could be simply estimated that $C_{max,u}$ of fluvastatin increases to C_{max} which is shown in Table 1. Further, high bilirubin concentration in patients with cirrhosis could increase unbound drug concentration, because bilirubin is also has high affinity to albumin (Oettl et al., 2013). Although no previous report exist which mentioned about free concentrations in renal tubular lumen under pathological conditions, we simply discussed with important information for drug adjustment such as hypoalbuminemia in pathological condition and lower levels of albumin in dialysis patients. Therefore, we could estimate the inhibitory effects of drugs on OATP4C1 by using the IC_{50} values and DDI indices in patients with chronic disease states. Among the tested drugs, ritonavir showed the highest DDI index for OATP4C1 under low albumin conditions, indicating a strong possibility of clinical drug interactions in patients with chronic disease states.

Based on the previous studies of ritonavir, it was suggested that significant interactions could occur with drugs that are extensively metabolized by CYP3A (Hsu et al., 1998). For example, ritonavir increased the AUC of clarithromycin by 77% (Ouellet et al., 1998). Additionally, ritonavir almost completely inhibited the formation of 14-hydroxy-clarithromycin, which is formed by the metabolic enzyme CYP3A (Ouellet et al., 1998). Although several studies have revealed the impact of CYP3A-mediated metabolism on the pharmacokinetic alteration of drugs, other processes such as transcellular dynamics regulated by several transporters cannot be ignored. Ritonavir has been reported to have a high affinity for P-glycoprotein (P-gp) (Vermeer et

JPET Fast Forward. Published on May 26, 2017 as DOI: 10.1124/jpet.117.241703
This article has not been copyedited and formatted. The final version may differ from this version.

al., 2016). Clinically, it was reported that pre-treatment with saquinavir/ritonavir 1,000/100 mg twice daily increased digoxin exposure most likely via P-gp inhibition (Schmitt et al., 2010). Although previous reports have stated that CYP3A and P-gp were most likely molecules responsible for altered drug pharmacokinetics, those molecules cannot explain the whole drug interactions *in vivo*. Ritonavir showed the strongest interaction with OATP4C1 in the current study. Out of 53 drugs tested, only 3 (i.e., 5%) (ritonavir, quinidine and saquinavir) had DDI indices (C_{max}/IC_{50}) > 0.1. Our result is similar to the rate reported for OAT1 (35/727 compounds [5%]) and OAT3 (73/727 compounds [10%]) (Duan et al., 2012). In addition, these 3 drugs have all been shown to exhibit renal DDI with digoxin, supporting recent proposal from physiologically based pharmacokinetic (PBPK) modeling that uptake is rate limiting in digoxin renal excretion (Scotcher et al., 2017). It is possible that OATP4C1 plays an important role in the drug interactions shown above. Further study is needed to clarify the contribution of OATP4C1 to the well-known drug interactions seen in clinical practice.

In conclusion, we provided novel information about OATP4C1-based interactions between various therapeutic drugs. We also evaluated the possibility of OATP4C1 involvement in DDIs by using the IC_{50} values and DDI indices. OATP4C1 might have an important role in clinical therapy. Our findings will give a new insight into the investigations of DDI and drug development in the future.

Author Contributions

Participated in research design: Sato, Abe, and Yamaguchi.

Conducted experiments: Sato, Mishima, and Yamaguchi.

Performed data analysis: Sato, Mishima, and Yamaguchi.

Wrote or contributed to the writing of the manuscript: Sato, Mishima, Mano, Abe, and Yamaguchi.

References

Capucci A, Aschieri D, and Villani GQ (1998) Clinical pharmacology of antiarrhythmic drugs. Drugs Aging 13: 51-70.

Chen N and Reith ME (2007) Substrates and inhibitors display different sensitivity to expression level of the dopamine transporter in heterologously expressing cells. J Neurochem 101: 377-388.

Chioukh R, Noel-Hudson MS, Ribes S, Fournier N, Becquemont L, and Verstuyft C (2014) Proton pump inhibitors inhibit methotrexate transport by renal basolateral organic anion transporter hOAT3. Drug Metab Dispos 42: 2041–2048.

Chu XY, Bleasby K, Yabut J, Cai X, Chan GH, Hafey MJ, Xu S, Bergman AJ, Braun MP, Dean DC, and Evers R (2007) Transport of the dipeptidyl peptidase-4 inhibitor sitagliptin by human organic anion transporter 3, organic anion transporting polypeptide 4C1, and multidrug resistance P-glycoprotein. J Pharmacol Exp Ther 321: 673–683.

Duan P, Li S, Ai N, Hu L, Welsh WJ, and You G (2012) Potent inhibitors of human organic anion transporters 1 and 3 from clinical drug libraries: discovery and molecular characterization. Mol Pharm 9: 3340-3346.

FDA (2012) Drug interaction studies—study design, data analysis, implications for dosing, and labeling recommendations. FDA, Rockville, MD. http://www.fda.gov/downloads/Drugs/Guidances/ucm292362.pdf.

Forette F, Bellet M, Henry JF, Hervy MP, Poyard-Salmeron C, Bouchacourt P, and Guerret M (1985) Effect of nicardipine in elderly hypertensive patients. Br J Clin Pharmacol 20:

125S-129S.

Fujiwara Y, Hamada A, Mizugaki H, Aikawa H, Hata T, Horinouchi H, Kanda S, Goto Y, Itahashi K, Nokihara H, Yamamoto N, and Ohe Y (2016) Pharmacokinetic profiles of significant adverse events with crizotinib in Japanese patients with ABCB1 polymorphism. Cancer Sci 107: 1117-1123.

Hagenbuch B and Meier PJ (2003) The superfamily of organic anion transporting polypeptides. Biochim Biophys Acta 1609: 1–18.

Hagenbuch B and Meier PJ (2004) Organic anion transporting polypeptides of the OATP/ SLC21 family: phylogenetic classification as OATP/ SLCO superfamily, new nomenclature and molecular/functional properties. Pflugers Arch 447: 653–665.

Hsu A, Granneman GR, and Bertz RJ (1998) Ritonavir. Clinical pharmacokinetics and interactions with other anti-HIV agents. Clin Pharmacokinet 35: 275-291.

Ito K, Iwatsubo T, Kanamitsu S, Ueda K, Suzuki H, and Sugiyama Y (1998) Prediction of pharmacokinetic alterations caused by drug-drug interactions: metabolic interaction in the liver. Pharmacol Rev 50: 387–412.

Izumi S, Nozaki Y, Maeda K, Komori T, Takenaka O, Kusuhara H, and Sugiyama Y (2015) Investigation of the impact of substrate selection on in vitro organic anion transporting polypeptide 1B1 inhibition profiles for the prediction of drug-drug interactions. Drug Metab Dispos 43: 235–247.

Krecic-Shepard ME, Barnas CR, Slimko J, Jones MP, and Schwartz JB (2000) Gender-specific effects on verapamil pharmacokinetics and pharmacodynamics in humans. J Clin Pharmacol

40: 219-230.

Kullak-Ublick GA, Stieger B, and Meier PJ (2004) Enterohepatic bile salt transporters in normal physiology and liver disease. Gastroenterology 126: 322–342.

Landersdorfer CB, Kirkpatrick CM, Kinzig M, Bulitta JB, Holzgrabe U, Jaehde U, Reiter A, Naber KG, Rodamer M, and Sörgel F (2010) Competitive inhibition of renal tubular secretion of ciprofloxacin and metabolite by probenecid. Br J Clin Pharmacol 69: 167-178.

Laskin OL, de Miranda P, King DH, Page DA, Longstreth JA, Rocco L, and Lietman PS (1982) Effects of probenecid on the pharmacokinetics and elimination of acyclovir in humans. Antimicrob Agents Chemother 21: 804-807.

Lau YY, Huang Y, Frassetto L, and Benet LZ (2007) Effect of OATP1B transporter inhibition on the pharmacokinetics of atorvastatin in healthy volunteers. Clin Pharmacol Ther 81: 194–204.

Lu Y, Nakanishi T, and Tamai I (2013) Functional cooperation of SMCTs and URAT1 for renal reabsorption transport of urate. Drug Metab Pharmacokinet 28: 153-158.

Małgorzewicz S, Debska-Slizień A, Rutkowski B, and Lysiak-Szydłowska W (2008) Serum concentration of amino acids versus nutritional status in hemodialysis patients. J Ren Nutr 18: 239-247.

Meijers BK, Bammens B, Verbeke K, and Evenepoel P (2008) A review of albumin binding in CKD. Am J Kidney Dis 51: 839-850.

Mikkaichi T, Suzuki T, Tanemoto M, Ito S, and Abe T (2004a) The organic anion transporter (OATP) family. Drug Metab Pharmacokinet 19: 171–179.

Mikkaichi T, Suzuki T, Onogawa T, Tanemoto M, Mizutamari H, Okada M, Chaki T, Masuda S,

Tokui T, Eto N, Abe M, Satoh F, Unno M, Hishinuma T, Inui K, Ito S, Goto J, and Abe T (2004b) Isolation and characterization of a digoxin transporter and its rat homologue expressed in the kidney. Proc Natl Acad Sci U.S.A. 101: 3569–3574.

Oettl K, Birner-Gruenberger R, Spindelboeck W, Stueger HP, Dorn L, Stadlbauer V, and Putz-Bankuti C (2013) Oxidative albumin damage in chronic liver failure: relation to albumin binding capacity, liverdysfunction and survival. J Hepatol 59: 978-983.

Ouellet D, Hsu A, Granneman GR, Carlson G, Cavanaugh J, Guenther H, and Leonard JM (1998) Pharmacokinetic interaction between ritonavir and clarithromycin. Clin Pharmacol Ther 64: 355-362.

Overdiek HW, Hermens WA, and Merkus FW (1985) New insights into the pharmacokinetics of spironolactone. Clin Pharmacol Ther 38: 469-474.

Pan X, Wang L, Grundemann D, and Sweet DH (2013) Interaction of ethambutol with human organic cation transporters of the SLC22 family indicates potential for drug-drug interactions during antituberculosis therapy. Antimicrob Agents Chemother 57: 5053–5059.

Parvez MM, Kaisar N, Shin HJ, Jung JA, and Shin JG (2016) Inhibitory interaction potential of 22 antituberculosis drugs on organic anion and cation transporters of the SLC22A family. Antimicrob Agents Chemother 60: 6558-6567.

Rodvold KA (1999) Clinical pharmacokinetics of clarithromycin. Clin Pharmacokinet 37: 385-398.

Rodvold KA and Neuhauser M (2001) Pharmacokinetics and pharmacodynamics of fluoroquinolones. Pharmacotherapy 21: 233S-252S.

Rozga J, Piątek T, and Małkowski P (2013) Human albumin: old, new, and emerging applications. Ann Transplant 18: 205-217.

Sato T, Yamaguchi H, Kogawa T, Abe T and Mano N (2014) Organic anion transporting polypeptides 1B1 and 1B3 play an important role in uremic toxin handling and drug-uremic toxin interactions in the liver. J Pharm Pharm Sci 17: 475-484.

Sato T, Ito H, Hirata A, Abe T, Mano N, and Yamaguchi H (2017) Interactions of crizotinib and gefitinib with organic anion-transporting polypeptides (OATP)1B1, OATP1B3, and OATP2B1: gefitinib shows contradictory interaction with OATP1B3. Xenobiotica, in press. DOI: 10.1080/00498254.2016.1275880

Schmitt C, Kaeser B, Riek M, Bech N, and Kreuzer C (2010) Effect of saquinavir/ritonavir on P-glycoprotein activity in healthy volunteers using digoxin as a probe. Int J Clin Pharmacol Ther 48: 192-199.

Scotcher D, Jones CR, Galetin A, and Rostami-Hodjegan A (2017) Delineating the Role of Various Factors in Renal Disposition of Digoxin through Application of Physiologically Based Kidney Model to Renal Impairment Populations. J Pharmacol Exp Ther 360: 484-495.

Scripture CD and Pieper JA (2001) Clinical pharmacokinetics of fluvastatin. Clin Pharmacokinet 40: 263-281.

Suga T, Yamaguchi H, Sato T, Maekawa M, Goto J, and Mano N (2017) Preference of conjugated bile acids over unconjugated bile acids as substrates for OATP1B1 and OATP1B3. PLoS One 12: e0169719.

Toyohara T, Suzuki T, Morimoto R, Akiyama Y, Souma T, Shiwaku HO, Takeuchi Y, Mishima E,

Abe M, Tanemoto M, Masuda S, Kawano H, Maemura K, Nakayama M, Sato H, Mikkaichi T, Yamaguchi H, Fukui S, Fukumoto Y, Shimokawa H, Inui K, Terasaki T, Goto J, Ito S, Hishinuma T, Rubera I, Tauc M, Fujii-Kuriyama Y, Yabuuchi H, Moriyama Y, Soga T, and Abe T (2009) SLCO4C1 transporter eliminates uremic toxins and attenuates hypertension and renal inflammation. J Am Soc Nephrol 20: 2546–2555.

Vermeer LM, Isringhausen CD, Ogilvie BW, and Buckley DB (2016) Evaluation of ketoconazole and its alternative clinical CYP3A4/5 inhibitors as inhibitors of drug transporters: the in vitro effects of ketoconazole, ritonavir, clarithromycin, and itraconazole on 13 clinically-relevant drug transporters. Drug Metab Dispos 44: 453-459.

Viani A, Carrai M, and Pacifici GM (1989) Plasma protein binding of frusemide in liver disease: effect of hypoalbuminaemia and hyperbilirubinaemia. Br J Clin Pharmacol 28: 175-178.

Vree TB, van den Biggelaar-Martea M, and Verwey-van Wissen CP (1995) Probenecid inhibits the renal clearance of frusemide and its acyl glucuronide. Br J Clin Pharmacol 39: 692-695.

Yamaguchi H, Sugie M, Okada M, Mikkaichi T, Toyohara T, Abe T, Goto J, Hishinuma T, Shimada M, and Mano N (2010) Transport of estrone 3-sulfate mediated by organic anion transporter OATP4C1: estrone 3-sulfate binds to the different recognition site for digoxin in OATP4C1. Drug Metab Pharmacokinet 25: 314-317.

Yang CH, Glover KP, and Han X (2009) Organic anion transporting polypeptide (Oatp) 1a1-mediated perfluorooctanoate transport and evidence for a renal reabsorption mechanism of Oatp1a1 in renal elimination of perfluorocarboxylates in rats. Toxicol Lett 190: 163-171.

Yonezawa A and Inui K (2011) Organic cation transporter OCT/SLC22A and H(+)/organic cation

antiporter MATE/SLC47A are key molecules for nephrotoxicity of platinum agents.Biochem Pharmacol 81: 563-568.

Footnotes

This work was supported by Japan Society for the Promotion of Science KAKENHI [Grant Number 23790168 (Hiroaki Yamaguchi), 15H00485 (Toshihiro Sato).]

JPET Fast Forward. Published on May 26, 2017 as DOI: 10.1124/jpet.117.241703
This article has not been copyedited and formatted. The final version may differ from this version.

Figure legends

Figure 1. Characterization of newly established OATP4C1-expressing MDCKII cells. (A) Samples were harvested 10 min after addition of T_3 (1 μM) to cells in order to monitor the level of T_3 uptake. A comparison was made between the uptake of T_3 into OATP4C1-expressing MDCKII cells with and without 5 mM sodium butyrate. Results are expressed as the mean ± standard error (S.E.), (n = 3). An asterisk indicates a significant difference from the value of the cells without 5 mM sodium butyrate ($p < 0.05$). (B) Immunoblotting of OATP4C1 expressed in MDCKII cells with or without 5 mM sodium butyrate. The band at 95~135 kDa (arrow head) represents OATP4C1. (C, D) Fluorescence microscopy of OATP4C1 expressed in MDCKII cells with or without 5 mM sodium butyrate. OATP4C1 proteins were observed in OATP4C1-transfected MDCKII cells (OATP4C1 proteins were stained in red). Nuclei were stained with DAPI in blue. Scale bars = 10 μm. (D) OATP4C1 appears at the cell surface membrane in the presence of 5 mM sodium butyrate.

Figure 2. Effects of various therapeutic drugs on T_3 uptake by OATP4C1-expressing MDCKII cells. Cells were incubated for 10 min at 37°C with 1 μM T_3 in the presence or absence of the trial drugs. Drug concentrations were as follows; 100 μM mycophenolic acid, 100 μM ranitidine, 100 μM rabeprazole, 100 μM lansoprazole, 100 μM diclofenac, 100 μM naproxen, 100 μM indomethacin, 50 μM celecoxib, 100 μM propranolol, 100 μM nicardipine, 100 μM nifedipine, 100 μM hydralazine, 100 μM candesartan, 100 μM losartan, 100 μM captopril, 100 μM hydrochlorothiazide, 100 μM furosemide, 100 μM spironolactone, 100 μM bosentan, 100 μM

JPET Fast Forward. Published on May 26, 2017 as DOI: 10.1124/jpet.117.241703
This article has not been copyedited and formatted. The final version may differ from this version.

tolbutamide, 100 μM fexofenadine, 100 μM diphenhydramine, 50 μM pravastatin, 50 μM fluvastatin, 50 μM gefitinib, 50 μM crizotinib, 100 μM imatinib, 100 μM lenalidomide, 1000 μM penicillin G, 1000 μM levofloxacin, 100 μM sparfloxacin, 100 μM cefaclor, 1000 μM cefazolin, 100 μM vancomycin, 100 μM daptomycin, 250 μM clarithromycin, 100 μM erythromycin, 25 μM itraconazole, 1000 μM fluconazole, 1000 μM sulfamethoxazole, 100 μM trimethoprim, 100 μM ritonavir, 25 μM saquinavir, 100 μM valaciclovir, 1000 μM acyclovir, 100 μM rifampicin, 100 μM amiodarone, 100 μM cibenzoline, 100 μM verapamil, 100 μM quinidine, 100 μM warfarin, 1000 μM probenecid and 100 μM empagliflozine. OATP4C1-mediated transport was calculated after by taking the total cellular uptake by OATP4C1-expressing cells and subtracting nonspecific uptake by mock cells. Each point and bar represents the mean ± standard error (S.E.). An asterisk indicates a significant difference from the value of the drug-naïve cells ($p < 0.05$).

Figure 3. Inhibitory effects of 10 drugs on OATP4C1-mediated T_3 uptake. Cells were incubated for 10 min at 37°C with 1 μM T_3 in the presence or absence of (A) nicardipine (0.3-100 μM), (B) spironolactone (0.3-100 μM), (C) fluvastatin (0.3-100 μM), (D) crizotinib (0.1-30 μM), (E) levofloxacin (10-3000 μM), (F) clarithromycin (1-300 μM), (G) ritonavir (0.3-100 μM), (H) saquinavir (0.1-30 μM), (I) quinidine (1-300 μM), and (J) verapamil (3-1000 μM). OATP4C1-mediated transport was calculated after by taking the total cellular uptake by OATP4C1-expressing cells and subtracting nonspecific uptake by mock cells. Each point and bar represents the mean ± standard error (S.E.). The data are shown as a percentage of the transport done by the control. Solid lines represent fitted lines for the inhibition of T_3 uptake by the

JPET Fast Forward. Published on May 26, 2017 as DOI: 10.1124/jpet.117.241703
This article has not been copyedited and formatted. The final version may differ from this version.

inhibitors that were obtained by a nonlinear least-squares regression analysis based on equation (1).

JPET Fast Forward. Published on May 26, 2017 as DOI: 10.1124/jpet.117.241703
This article has not been copyedited and formatted. The final version may differ from this version.

Table 1. Drug-drug interaction (DDI) indices estimated from *in vitro* OATP4C1-mediated T_3 uptake inhibition kinetics by therapeutic drugs.

					DDI index	
Drug	IC_{50} (μM)	C_{max} (μM)	$C_{max,u}$ (μM)	$f_{max,u}$ (%)	$[I] = [I]_{max}$	$[I] = [I]_{max,u}$
Levofloxacin	420 ± 150	19 [1)]	14.1	74 [1)]	0.045	0.033
Ritonavir	8.5 ± 1.4	16 [2)]	0.16	1 [2)]	1.9	0.019
Quinidine	100 ± 11	19 [3)]	1.9	10 [3)]	0.19	0.019
Saquinavir	4.3 ± 0.6	3.7 [2)]	0.074	2 [2)]	0.86	0.0172
Clarithromycin	200 ± 16	3.8 [4)]	1.9	50 [4)]	0.019	0.0095
Crizotinib	24 ± 8	1.1 [5)]	0.099	9 [5)]	0.046	0.0041
Spironolactone	53 ± 7	0.48 [6)]	0.048	10 [6)]	0.0091	0.00091
Fluvastatin	41 ± 8	0.65 [7)]	0.033	5 [7)]	0.016	0.00079
Nicardipine	51 ± 8	0.27 [8)]	0.027	10 [8)]	0.0053	0.00053
Verapamil	110 ± 22	0.51 [9)]	0.051	10 [9)]	0.0046	0.00046

IC_{50} (μM) are shown as mean ± S.E., $f_{max,u}$ (%) is the unbound fraction of the drugs.
Data for C_{max} and $f_{max,u}$ (%) of the drugs are from previous reports.
The DDI indices were determined using the inhibition constant (IC_{50}) with the maximum plasma concentration (C_{max}; bound plus unbound) ($[I]_{max}$) and the maximum unbound concentration ($C_{max,u}$) ($[I]_{max,u}$) of the drugs following the regulatory guidelines described in the text.
The values were obtained from references shown below;
1) Rodvold and Neuhauser, 2001; 2) Hsu et al., 1998; 3) Capucci et al., 1998; 4) Rodvold, 1999; 5) Fujiwara et al., 2016; 6) Overdiek et al., 1985; 7) Scripture and Pieper, 2001; 8) Forette et al., 1985; 9) Krecic-Shepard et al., 2000

JPET Fast Forward. Published on May 26, 2017 as DOI: 10.1124/jpet.117.241703
This article has not been copyedited and formatted. The final version may differ from this version.

Figure 1

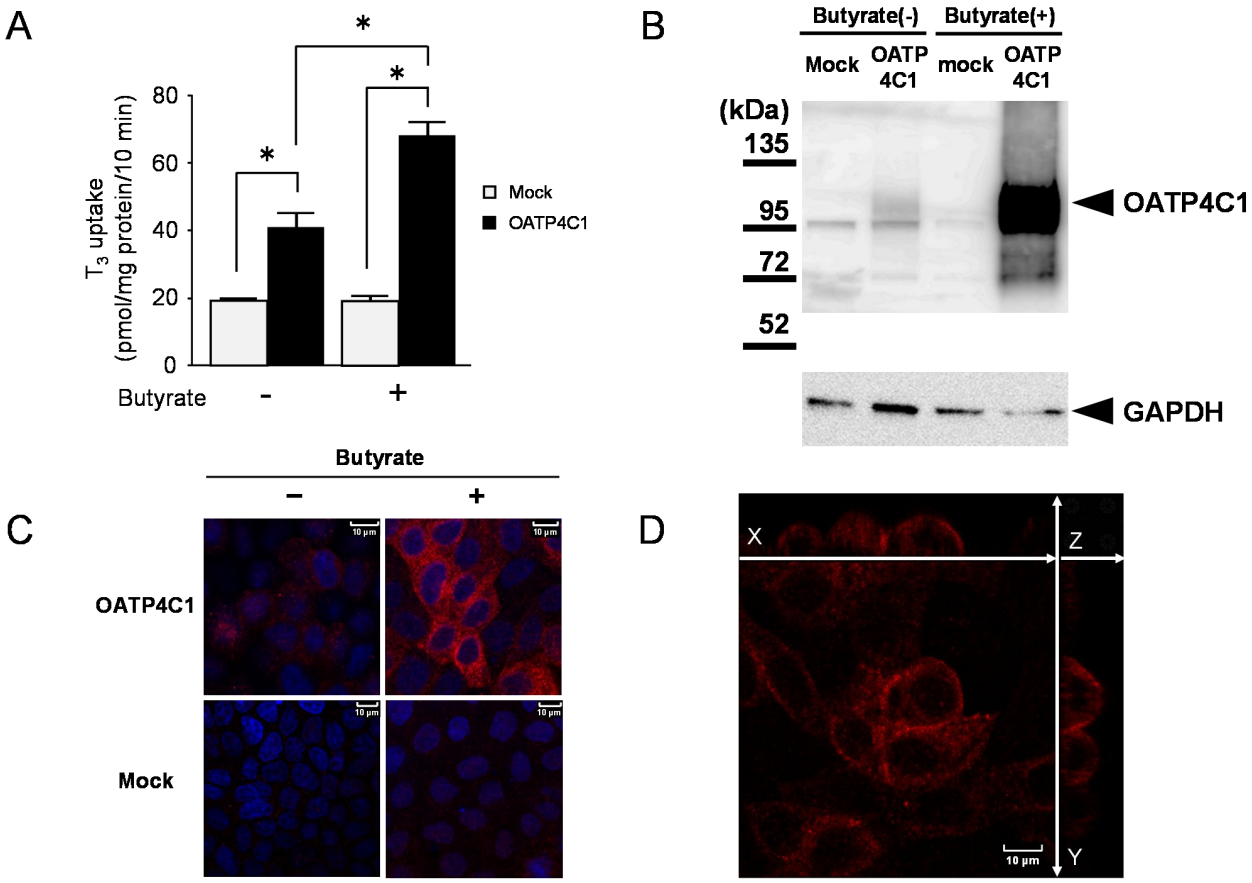

Figure 2

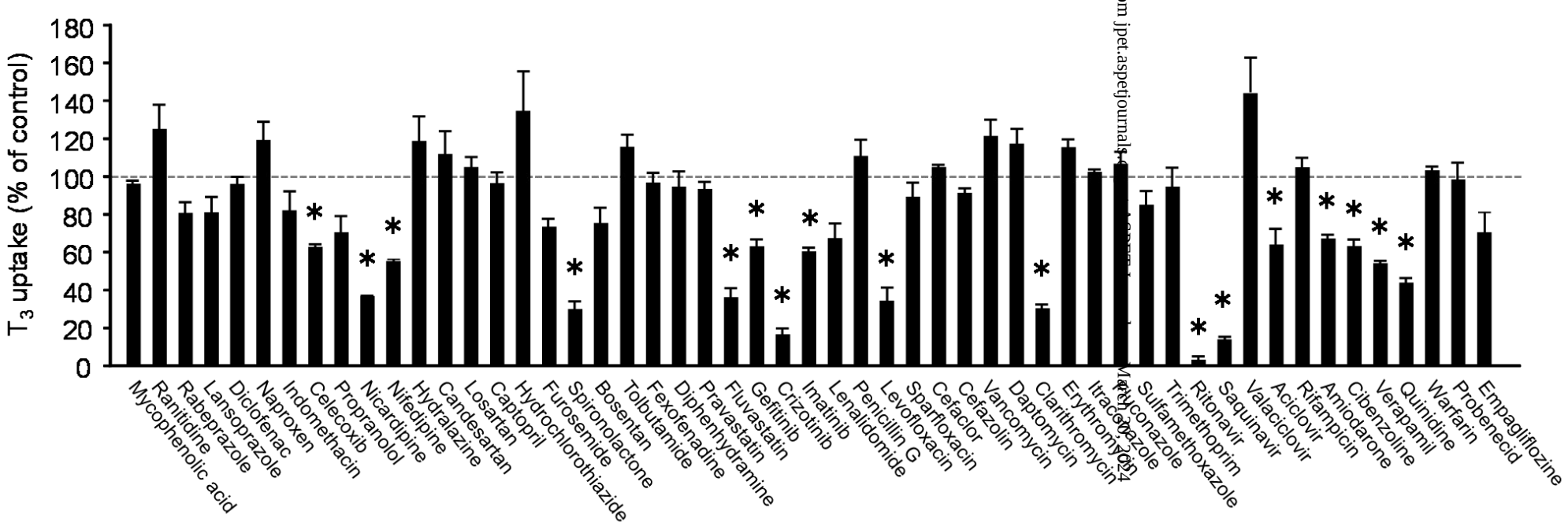

JPET Fast Forward. Published on May 26, 2017 as DOI: 10.1124/jpet.117.241703
This article has not been copyedited and formatted. The final version may differ from this version.

Figure 3